Fully Adaptive Distributionally Robust Multi-stage Framework for Uncertain Unit Commitment Based on Mixed Decision Rules

Linfeng Yang, *Member, IEEE*, Ying Yang, and Zhaoyang Dong, *Fellow, IEEE*

***Abstract*—With growing penetration of wind power into the power grid, while achieving low cost sustainable electricity supply, it also introduces technical challenges with the associated intermittency. This paper proposes a fully adaptive Wasserstein-based distributionally robust multi-stage framework based on mixed decision rules (MDR) for uncertain unit commitment problem (UUC) to better adapt wind power respecting non-anticipativity both in unit state decision and dispatch process. Comparing with the existing multi-stage model, the proposed framework introduces an improved MDR to handle all decision variables to expand feasible region, thus, this framework can obtain various typical models by adjusting the number of relevant periods of decision variables. As a result, our model can find feasible solution to some problems that are not feasible in the traditional models while finding better solution to feasible problems. The proposed model is reformulated with advanced optimization method and improved MDR to form the mixed integer linear programming (MILP) model to address the computational intractability. The effectiveness and efficiency of the proposed model have been validated with case studies using IEEE benchmark systems.**

***Index Terms*—mixed decision rules (MDR), multi-stage, non-anticipativity, distributionally robust optimization (DRO), uncertain unit commitment (UUC), wind power.**

NOMENCLATURE

Indices:

i, j	Index for unit/bus/wind generator.
t	Index for time period.

Constants:

N	Total number of units.
T	Total number of time periods.
R	Total number of wind generators.
S^{W}	Set of buses with wind generators, $\lvert S^{\mathrm{W}}\rvert = R$ and $S^{\mathrm{W}} = \{1, \dots, R\}$.
S^{B}	Set of buses, $\lvert S^{\mathrm{B}}\rvert = N$ and $S^{\mathrm{B}} = \{1, \dots, N\}$.
S^{G}	Set of buses with units. $\lvert S^{\mathrm{G}}\rvert = G$ and $S^{\mathrm{G}} \subseteq S^{\mathrm{B}}$.
S^{TP}	Set of time periods, and $\lvert S^{\mathrm{TP}}\rvert = T$.
S^{L}	Set of lines, and $\lvert S^{\mathrm{L}}\rvert = L$.
S^{ref}	Set of reference bus.
a_i, b_i, c_i	Coefficients of the quadratic production cost function of unit i.
$C_{\mathrm{cold},i}, C_{\mathrm{hot},i}$	Cold and hot startup cost of unit i.
$T_{\mathrm{cold},i}$	Cold startup time of unit i.
$\underline{P}_i, \overline{P}_i$	Minimum and maximum power output of unit i.
$P_{\mathrm{D},t}$	System load demand in period t.
R_t	Spinning reserve requirement in period t.
$P_{\mathrm{up},i}, P_{\mathrm{down},i}$	Ramp up and ramp down limit of unit i.
$P_{\mathrm{start},i}, P_{\mathrm{shut},i}$	Startup and shutdown ramp limit of unit i.
$u_{i,0}$	Initial commitment state of unit i.
$T_{i,0}$	Number of periods unit i has been online $(+)$ or offline $(-)$ prior to the first period of the time span (end of period 0).
$\underline{T}_{\mathrm{on},i}, \underline{T}_{\mathrm{off},i}$	Minimum up and minimum down time of unit i.
U_i	$\left[\min\left[T, u_{i,0}\left(\underline{T}_{\mathrm{on},i} - T_{i,0}\right)\right]\right]^+$
L_i	$\left[\min\left[T, (1-u_{i,0})\left(\underline{T}_{\mathrm{off},i} + T_{i,0}\right)\right]\right]^+$
τ_i	$\max\left(t - \underline{T}_{\mathrm{off},i} - T_{\mathrm{cold},i}, 1\right)$
$f_{i,t}$	$\begin{cases} 1, (t-\tau_i \le 0) \,\&\, \left(\left[-T_{i,0}\right]^+ < \lvert t-\tau_i\rvert + 1\right) \\ 0, \text{otherwise} \end{cases}$
C^l	Value of load loss.
$\underline{l}^{\mathrm{D}}_{i,t}, \overline{l}^{\mathrm{D}}_{i,t}$	Minimum and maximum load loss on bus i in time period t.

Variables:

$u_{i,t}$	On/off status of unit i in period t.
$s_{i,t}$	Startup status of unit i in period t.
$d_{i,t}$	Shutdown status of unit i in period t.
$\tilde{S}_{i,t}$	The part of startup cost of unit i in period t exceeding $C_{\mathrm{hot},i}$.
$l^{\mathrm{D}}_{i,t}$	Load loss at bus i during time period t.
$P^{\mathrm{G}}_{i,t}$	Power output of unit on bus i in time period t.
$\boldsymbol{P}$	$\left[P^{\mathrm{G}}_{[i\in S^{\mathrm{G}}],[t\in S^{\mathrm{TP}}]}\right]^{\mathrm{T}}$.
$\theta_{i,t}$	Phase angle on bus i in time period t.
$\boldsymbol{\theta}$	$\left[\theta_{[i\in S^{\mathrm{B}}],[t]}\right]^{\mathrm{T}}$

Operator:

$\{\cdot\}^+$	$\max(0,\cdot)$
$\mathbb{I}(\cdot)$	the indicator function
$[\cdot]$	$\{1,2,\dots,\cdot\}$
$[\cdot]^\wedge$	$\{0,1,2,\dots,\cdot\}$

This work was supported by the Natural Science Foundation of Guangxi (2020GXNSFAA297173, 2020GXNSFDA238017, 2021GXNSFBA075012), the Natural Science Foundation of China (51767003, 71861002). (Corresponding author: Linfeng Yang)

L.F. Yang and Y. Yang are with the School of Computer Electronics and Information, Guangxi University, Nanning 530004, China. And L.F. Yang is also with the Guangxi Key Laboratory of Multimedia Communication and Network Technology, Guangxi University. (email: ylf@gxu.edu.cn, 907803678@qq.com).

Z.Y Dong is with School of Electrical and Electronics Engineering, Nanyang Technological University, Singapore. (e-mail: zydong@ieee.org)

$[x; y]$ $\begin{bmatrix} x \\ y \end{bmatrix}$
$\xi_{[\cdot]}$ $[\xi_1; \xi_2; \dots, \xi_\cdot]$ or $[\xi_1, \xi_2, \dots, \xi_\cdot]$
$i{:}j$ $\{i, i+1, \dots, j\}$

I. Introduction

The aim of typical unit commitment (UC) is to minimize the generator's fuel consumption or the operation cost of whole system by scheduling generators [1]. Recently, higher and higher penetration of renewable energy resources into UC problem to address energy crisis and increasing impact of greenhouse gas emission on global warming [2]-[4], wind energy is the most widely used among them due to its free availability and environment friendliness [4], [5]. Despite the above advantages, integrating wind power into power system presents a formidable challenge since its intermittency and volatility, which makes the UC model a large-scale and uncertain problem [6], [7].

Fortunately, there are two effective solutions to above challenges: wind power forecast [8], [9] and optimization methods for the uncertain UC problem (UUC). The forecasting errors will be appropriately modeled with the introduction of different approaches, an ensemble pruning and combination problem is formulated in [8], which can enhance short-term prediction. Abdollah et al. proposed a new lower upper bound estimation method to construct prediction intervals to capture the uncertainty [9]. Notwithstanding, these deterministic methods cannot completely meet the decision-making requirements in an uncertain environment. On the other hand, in recent years, optimization methods have been representative method as its practical significance of UUC, there are three main approaches [6]: robust optimization (RO), stochastic optimization (SO) and distributionally robust optimization (DRO). RO can guarantee the robustness of the scheduling scheme by optimizing the worst-case in the uncertainty set [10] and SO maximizes profits by assuming that its distribution is the real distribution [11]. However, the security constraints of SO may be breached because of the unreliable probability distribution while RO always obtains an over-conservative scheduling scheme in real scenario.

Therefore, DRO demonstrates significant superiority over other methods for it can weigh the radicalism of SO and the conservatism of RO, all probability distributions of DRO's ambiguity set have been immunized by finding and optimizing the worst-case in the possible distribution family [12]. After years of research and development, DRO, especially moment-based DRO [13], [14] has been used in many fields, such as energy systems and UC, nevertheless, these moment-based DRO also has the drawbacks. Firstly, it cannot guarantee that the unknown distribution will converge to the true distribution, furthermore, the only utilization of moment information is still conservative. Motivated by above facts, references [12], [15]-[17] developed a new method called distance-based DRO, where the ambiguity set consisted of the distributions within a fixed distance from the nominal distribution. [12] provides a Wasserstein-based DRO and its approximate framework, which can manage the risk from wind power forecasted errors and minimize the generating cost. The authors in [15] proposed a min-max-min KL-based DRO to control the expected cost in the worst case. A chance constrained optimal power flow model for UUC was introduced by [16].

A class of two-stage models were developed in [18], [19]. Under the two-stage model, the day-ahead unit state decision is made at stage 1, and the real-time dispatch decision is made at stage 2 across the scheduling horizon. Stage 2's decisions are made based on the complete knowledge of uncertain variables cross the entire operating periods whereas the decisions are actually made sequentially in engineering practices because generation dispatch of each hour only depends on the information of the realised uncertain variables up to that hour. To improve the deficiency of two-stage, multi-stage models were introduced in [18]-[21], where the state of unit decisions are *here-and-now*, i.e. Made day-ahead, and the hourly dispatch decisions of the next day are made on *wait-and-see* basis. This demonstrates the non-anticipativity for the sequential observation of uncertainties. However, most multi-stage models are generally intractable to solve, an effect approach to approximately overcome this problem are decision rules, which choosing some real-valued functions with pre-specified structures [13], [22]. Reference [23] first used the decision rules for real-valued functions in 1974. Linear/affine decision rule's real-valued functions are employed as linear function of uncertain variables in [24]. These approaches are direct and crude. The non-linear decision rule used in [25] enables the real-valued adaptive decisions parameterised by a nonlinear lifting operator to define the structure of the decision rule. [18] use simplified affine policies to construct a more solvable structure. Linear decision rules utilized in multi-stage models to ensure the computational tractability in [19]. T. Ding *et al*. [21] designed a stochastic dual dynamic programming-based decomposition method to handle the computation intractability.

The above multi-stage models are still some flaws, although these models use a rolling optimization to dispatch generation to accommodate uncertain variables, the state of units are still fixed. Thus, if the uncertain variable fluctuates greatly, there may be no feasible dispatch scheme that can adapt to the uncertain variable in any given unit state, that is, no feasible solution can be find in the scenario, which motivates us to consider more adaptive DRO model. Accordingly, we propose a fully adaptive multi-stage distributionally robust framework based on mixed decision rules for UUC (DR-MDR), which provides a larger feasible region and results a better optimal solution than traditional deterministic models and multi-stage models. The main contributions can be summarized as:

1) A fully adaptive multi-stage distributionally robust framework based on Wasserstein-metric and mixed decision rules is proposed for the UUC, respecting non-anticipativity both in unit state decision and dispatch process. Such a fully adaptive framework can not only get those traditional models by adjusting the number of relevant periods of decision variables, but also get a much more advanced model with larger feasible region, which has two merits: It can find the feasible solution to some problem that the traditional models is not feasible, and find a better solution for the problem that the

traditional models are feasible.

2) We use binary decision rules and linear decision rules (mixed decision rules) to handle all decision variables including integers and continuities for further adapt decision variables to uncertainty, it provides a sequential decision-making process which is that the uncertain wind is observed at a given time and the decision variables are made immediately after this observation. Therefore, unit decisions and dispatch decisions are wait-and-see and change in response to wind.

3) We developed a mixed integer linear programming (MILP) reformulation for the DR-MDR based optimization theory to address the computation intractability, and we improve the decision rules to reformulation of equality constraints, while the extensive computational study of proposed model and existing multi-stage model on IEEE test system demonstrates the superiority of our model.

The rest of the paper is organized as follows. Section II presents the typical UUC models and their limitations. A fully adaptive multi-stage distributionally robust model based on mixed decision rules for UUC and its reformulation are proposed in Sections III. Case studies using the proposed model for the IEEE 6-bus and 30-bus system are given in Section IV. Finally, Section V concludes this article.

II. Typical UUC Models and Their Limitations

A. Description of uncertain UC

1) Objective function

The objective of the problem with uncertain wind power is to minimize the total cost which includes the following three parts:

The generation cost of a thermal unit $C_{i,t}^{FG}$ is described as a quadratic function:

$$C_{i,t}^{FG} = a_i + b_i P_{i,t}^{\mathrm{G}} + c_i \left(P_{i,t}^{\mathrm{G}}\right)^2, \tag{1}$$

Given parameter $\mathcal{L}$, then let $p_{i,l} = \underline{P}_i + l\,(\overline{P}_i - \underline{P}_i)/\mathcal{L}$ and $l = 0,1,2,\dots,\mathcal{L}-1$, after replacing $C_{i,t}^{FG}$ with auxiliary variable $z_{i,t}$, then replacing Eq. (1) with the following linear constraints:

$$z_{i,t} \geq \left(2c_i p_{i,l} + b_i\right) C_{i,t}^{FG} + \left(a_i - \gamma_i \left(p_{i,l}\right)^2\right) u_{i,t}, \tag{2}$$

The startup cost of thermal unit $C_{i,t}^{ST}$, including hot startup cost $C_{i,t}^{HS}$ and excess of hot startup cost $C_{i,t}^{ES}$, which is

$$C_{i,t}^{ST} = C_{i,t}^{HS} + C_{i,t}^{ES}, \tag{3}$$

where

$$C_{i,t}^{ES} = C_{\mathrm{hot},i} s_{i,t}, \tag{4}$$

$$C_{i,t}^{ES} \geq \left(C_{\mathrm{cold},i} - C_{\mathrm{hot},i}\right)\left[s_{i,t} - \sum_{\tau_i}^{t-1} d_{i,\tau} - f_{i,t}\right], \tag{5}$$

$$C_{i,t}^{ES} \geq 0. \tag{6}$$

And the cost of load loss C^{CL}:

$$C^{CL} = \sum_{t\in S^{\mathrm{TP}}} \sum_{i\in S^{\mathrm{B}}} C^{l} l_{i,t}^{\mathrm{D}}, \tag{7}$$

Thus, the objective function are as follows:

$$f(\cdot) = \sum_{t\in S^{\mathrm{TP}}} \sum_{i\in S^{\mathrm{G}}} \left(C_{i,t}^{FG} + C_{i,t}^{ST}\right) + C^{CL}. \tag{8}$$

2) Thermal unit constraints

$$u_{i,t}\underline{P}_i \leq P_{i,t}^{\mathrm{G}} \leq u_{i,t}\overline{P}_i, \tag{9}$$

$$P_{i,t}^{\mathrm{G}} - P_{i,t-1}^{\mathrm{G}} \leq u_{i,t-1} P_{i,\mathrm{up}} + s_{i,t} P_{i,\mathrm{start}}, \tag{10}$$

$$P_{i,t-1}^{\mathrm{G}} - P_{i,t}^{\mathrm{G}} \leq u_{i,t} P_{i,\mathrm{down}} + d_{i,t} P_{i,\mathrm{shut}}. \tag{11}$$

where $\forall i \in S^{\mathrm{G}}, \forall t \in S^{\mathrm{TP}}$. Eq. (9) is the capacity limits of thermal units, Eq. (10)-(11) enforce ramp up/down limits of individual unit.

3) Binary variables constraints

$$u_{i,t} = u_{i,0}, \tag{12}$$

$$\sum_{\varpi=[t-\underline{T}_{\mathrm{on},i}]^+ +1}^{t} s_{i,\varpi} \leq u_{i,t}, \tag{13}$$

$$\sum_{\varpi=[t-\underline{T}_{\mathrm{off},i}]^+ +1}^{t} d_{i,\varpi} \leq 1 - u_{i,t}, \tag{14}$$

$$s_{i,t} - d_{i,t} = u_{i,t} - u_{i,t-1}, t \in S^{\mathrm{TP}}. \tag{15}$$

Eq. (12)-(14) $\forall i \in S^{\mathrm{G}}, t \in [L_i + 1, \dots, T]$. Eq. (12) is the initial status of units, Eq. (13) and Eq. (14) define minimum on/off time, and Eq. (15) denotes the state equality constraint of units.

4) System constraints

$$\underline{l}_{i,t}^{\mathrm{D}} \leq l_{i,t}^{\mathrm{D}} \leq \overline{l}_{i,t}^{\mathrm{D}}, \forall i \in S^{\mathrm{B}}, \tag{16}$$

$$P_{i,t}^{\mathrm{G}} + P_{i,t}^{\mathrm{W}} - P_{i,t}^{\mathrm{D}} + l_{i,t}^{\mathrm{D}} = \sum_{j\in S_{\mathrm{B}}} B_{ij}\theta_{j,t}, \forall i \in S^{\mathrm{B}}, \tag{17}$$

$$\theta_{i,t} = 0, \forall i \in S^{\mathrm{ref}}, \tag{18}$$

$$\left|\frac{\theta_{i,t} - \theta_{j,t}}{X_{ij}}\right| \leq F_{ij}^{\max}, \forall ij \in S^{\mathrm{L}}. \tag{19}$$

where $\forall t \in S^{\mathrm{TP}}$. Eq. (16) and (19) are the limitation of load loss and transmission lines, respectively, Eq. (17) represents the DC network model, and Eq. (18) denotes the reference bus.

5) Wind generators constraints

In this paper, $P_{i,t}^{\mathrm{W}}$ is used to denote the wind generation, which is equal to the expected value $\bar{P}_{i,t}^{\mathrm{W}}$ plus a random term representing forecast error $v_{i,t}^{\mathrm{W}}$:

$$P_{i,t}^{\mathrm{W}} \leq \bar{P}_{i,t}^{\mathrm{W}} + v_{i,t}^{\mathrm{W}}, \forall i \in S^{\mathrm{W}}, \forall t \in S^{\mathrm{TP}}. \tag{20}$$

We obtain the UUC problem:

$$\min f(\cdot) \tag{21}$$
$$s.t. \{(2)-(7), (9)-(20)\}.$$

B. Typical Two-stage UUC

The popular DRO or robust optimization UUC model [13], [18], [19] can be represented by typical two-stage formula.

$$\min_{\boldsymbol{x}\in\mathcal{X}} \left\{ \sum_{t=1}^{T} [\boldsymbol{c}_t^{\mathrm{T}} \boldsymbol{x}_t] + \min_{\boldsymbol{y}\in\mathcal{Y}(\boldsymbol{x},\boldsymbol{v}^{\mathrm{W}})} \sup_{\mathbb{P}^{\mathrm{W}}\in\Upsilon^{\mathrm{W}}} \mathbb{E}_{\mathbb{P}^{\mathrm{W}}} [\sum_{t=1}^{T} [\boldsymbol{d}_t^{\mathrm{T}} \boldsymbol{y}_t]] \right\}, \tag{22}$$

where $\boldsymbol{x}_t = \left[u_{[G],t}, s_{[G],t}, d_{[G],t}\right]$ denotes binary decision variables, $\boldsymbol{c}_t^{\mathrm{T}} \boldsymbol{x}_t = \sum_{i\in S^{\mathrm{G}}} C_{i,t}^{HS}$, $\mathcal{X} = \{x | (12)-(15)\}$ is the feasible constraints of $\boldsymbol{x}$, and $\boldsymbol{y}_t = \left[P_{[G],t}^{\mathrm{G}}, \theta_{[G],t}, z_{[G],t}, \tilde{S}_{[G],t}, P_{[W],t}^{\mathrm{W}}, l_{[N],t}^{\mathrm{D}}\right]$ denotes continuous decision variables, $\boldsymbol{d}_t^{\mathrm{T}} \boldsymbol{y}_t = \sum_{i\in S^{\mathrm{G}}} (z_{i,t} + C_{i,t}^{ES}) + \sum_{i\in S^{\mathrm{B}}} C_{i,t}^{CL}$, $\mathcal{Y}(\boldsymbol{x}, \boldsymbol{v}^{\mathrm{W}}) = \{y | (2), (5), (6), (9)-(11), (16)-(20)\}$ is the feasible constraints of $\boldsymbol{y}$ parameterized by the commitment decisions $\boldsymbol{x}$ and realized $\boldsymbol{v}^{\mathrm{W}}$, $\mathbb{P}^{\mathrm{W}}$ is a distribution of uncertainties $\boldsymbol{v}^{\mathrm{W}}$ and Υ^{W} is the ambiguity set.

The first-stage scheduling determines the unit status $\boldsymbol{x}$, before wind power is realized in the future, and the second-stage sub-problem determines the dispatch $\boldsymbol{y}$ after knowing wind power. Taking infinite space of the adaptive recourse function $\boldsymbol{y}(\boldsymbol{v}^{\mathrm{W}})$ to solve the problem is generally intractable to solve

[22].

C. Adaptive DRO UUC

Similar to Claim 1 and 2 of two-stage RO model in [18], the scheduling scheme obtained by model (22) can lead to infeasibility in the real-time application [19] because that, in the actual scenario, the dispatch decisions must be sequentially optimized in real-time with realized uncertainty observations prior to operating hour. To truly figure this process, the decision variables $\boldsymbol{y}_t$ should count on the history of wind power generation $\boldsymbol{v}_{[t]}^{\mathrm{w}} \coloneqq (\boldsymbol{v}_1^{\mathrm{w}}, \dots, \boldsymbol{v}_t^{\mathrm{w}})$, $\boldsymbol{v}_\tau^{\mathrm{w}} = \boldsymbol{v}_{[R],\tau}^{\mathrm{w}}$, $\tau \in [t]$, i.e., decision maker observes first wind power $\boldsymbol{\xi}_1$ and then makes first decision $\boldsymbol{y}_1(\cdot)$. Subsequently, second wind power $\boldsymbol{\xi}_2$ is revealed, in response, decision maker makes second decision $\boldsymbol{y}_2(\cdot)$. This alternating sequence of observations and decisions extends to T periods. Because of the above reasons, [19] develops an adaptive multi-stage DRO model by substituting $\boldsymbol{y}(\boldsymbol{v}^{\mathrm{w}})$ with $\left[\boldsymbol{y}_t\left(\boldsymbol{v}_{[t]}^{\mathrm{w}}\right), \forall t \in S^{\mathrm{TP}}\right]$ in (22), then it formulates the following adaptive DRO model:

$$\min_{\boldsymbol{x}\in\mathcal{X}}\left\{\sum_{t=1}^{T}[\boldsymbol{c}_t^{\mathrm{T}}\boldsymbol{x}_t] + \min_{\boldsymbol{y}_t(\cdot)\in\mathcal{Y}} \sup_{\mathbb{P}^{\mathrm{w}}\in\Upsilon^{\mathrm{w}}} \mathbb{E}_{\mathbb{P}^{\mathrm{w}}}[\sum_{t=1}^{T}[\boldsymbol{d}_t^{\mathrm{T}}\boldsymbol{y}_t(\cdot)]]\right\}, \quad (23)$$

The crucial feature of this adaptive multi-stage DRO model is the expression $y_t(\boldsymbol{v}_{[t]}^{\mathrm{w}})$, which respecting non-anticipativity by making the scheduling at time t is a function of wind power up to time t [19]. However, (23) still has drawback in some scenario, we will present a contrast flow chart and an example to epitomize the superiority of our framework over (23).

D. Typical model's limitations

Fig. 1 shows the difference in scheduling between the typical models and ours at a macro level. Furthermore, Fig. 2 gives the one-bus system structure, the system only has one period and one load bus A, which has both thermal unit and wind unit. Then, we assume the ambiguity is a single point set, the unit ramp constraints are ignored, wind power can be abandoned and load loss is not allowed. Nodal load $d_A = 20\mathrm{MW}$, wind generation $p_w \in [0,25]$ and thermal generation $p_A \in \{0, [15,20]\}$, the generation cost of thermal unit is 60/MW. $\xi \in [0, +\infty]$ is wind power.

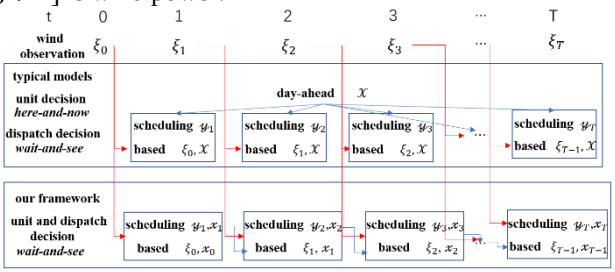

Fig. 1. Scheduling framework for typical models and ours.

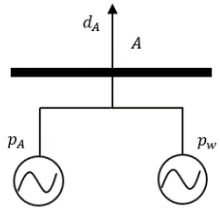

Fig. 2. Simple case to illustrate advantages of proposed model over typical multi-stage model (1-1 system).

Typical multi-stage model likes (23) need to fix the thermal unit commitment u before rolling scheduling, it is not difficult to find the system will be infeasible when $u = 0$ since the load d_A can only be satisfied when $p_w \geq 20$. Therefore, (23) fixes $u = 1$, in this case, thermal unit generation $p_A(\xi) = 15 + (5-\xi)^+$ and windy unit generation $p_w(\xi) = 5 - (5-\xi)^+$, the expectation of generation cost is $E_{obj} = (900 + 60 \times (5-\xi)^+) \in [900,1200]$.

In our framework, unit commitment u does not need to be fixed in advance but makes real-time decisions based on the wind power ξ. We have:

$$u(\boldsymbol{\xi}) = \begin{cases} 0, & \xi \geq 20 \\ 1, & else \end{cases}$$

In this case, thermal unit generation is $p_A(\xi) = \begin{cases} 0, & \xi \geq 20 \\ 15 + (5-\xi)^+, & else \end{cases}$ and windy unit generation is $p_w(\xi) = \begin{cases} \xi, & \xi \geq 20 \\ 5 - (5-\xi)^+, & else \end{cases}$, the expectation of generation cost is $E_{obj} = \left(\frac{20}{25}(900 + 60 \times (5-\xi)^+) + \frac{5}{20} \times 0\right) \in [720,960]$.

It can be seen from Fig. 1 and 2 that since the binary decision variable can also adapt to the wind power in real-time in our fully adaptive framework, the whole scheduling scheme is more willing to use the wind power, thus reducing the expectation of generation cost. More advantages of our proposed model will be delineated experimentally in Section IV.

III. The Proposed Fully Adaptive Framework

A. Fully Adaptive Framework

Here, we will introduce a sequential decision-making process in which uncertain wind power is observed at a given time, followed immediately (fully adaptive) by operational decisions (including $\boldsymbol{x}(\cdot)$ and $\boldsymbol{y}(\cdot)$) for a given period.

Therefore, our fully adaptive multi-stage DRO framework for UUC can be expressed by the following formula:

$$\min_{\boldsymbol{x}(\cdot),\boldsymbol{y}(\cdot)}\left\{\sup_{\mathbb{P}\in\Upsilon} \mathbb{E}_{\mathbb{P}}\left[\sum_{t=1}^{T}\left[\boldsymbol{c}_t^{\mathrm{T}}\boldsymbol{x}_t\left(\boldsymbol{\xi}_{[t_1]^\wedge}\right) + \boldsymbol{d}_t^{\mathrm{T}}\boldsymbol{y}_t\left(\boldsymbol{\xi}_{[t_2]^\wedge}\right)\right]\right]\right\} \quad (24)$$

$$\text{s.t.} \begin{cases} \sum_{\tau=1}^{t}\left[\boldsymbol{A}_\tau^t\boldsymbol{x}_\tau\left(\boldsymbol{\xi}_{[\tau_1]^\wedge}\right) + \boldsymbol{B}_\tau^t\boldsymbol{y}_\tau\left(\boldsymbol{\xi}_{[\tau_2]^\wedge}\right)\right] \leq \boldsymbol{D}^t\boldsymbol{\xi}_{[t]^\wedge} \\ \sum_{\tau=1}^{t}\left[\boldsymbol{\mathcal{A}}_\tau^t\boldsymbol{x}_\tau\left(\boldsymbol{\xi}_{[\tau_1]^\wedge}\right) + \boldsymbol{\mathcal{B}}_\tau^t\boldsymbol{y}_\tau\left(\boldsymbol{\xi}_{[\tau_2]^\wedge}\right)\right] = \boldsymbol{d}^t \end{cases} \forall \boldsymbol{\xi} \in \Xi, \forall t \in [T]$$

where $\boldsymbol{\xi} \coloneqq \left[\xi_{0,0} = 1; \xi_{i,t} = v_{i,t}^{\mathrm{w}}\right]$, $\xi_0 = \xi_{0,0}$, $\boldsymbol{\xi}_t = \xi_{[R],t}$, $t \in [T]$, $t_1 \leq t$, $t_2 \leq t$, $\tau_1 \leq \tau$, $\tau_2 \leq \tau$. The $\xi_{0,0}$ is introduced to represent affine functions of $\boldsymbol{v}^{\mathrm{w}}$ in a compact manner as linear functions of $\boldsymbol{\xi}$ [31], and $\boldsymbol{A}_\tau^t$, $\boldsymbol{B}_\tau^t$, $\boldsymbol{D}^t$, $\boldsymbol{\mathcal{A}}_\tau^t$, $\boldsymbol{\mathcal{B}}_\tau^t$, and $\boldsymbol{d}^t$ are the coefficient matrices/vectors associated with the constraint in time period t. $\mathbb{P}$ is the probability distribution of $\boldsymbol{\xi}$ which satisfied $\mathbb{P}(A) \coloneqq \mathbb{P}^{\mathrm{w}}\left(\left\{\boldsymbol{\xi}_{[T]} \middle| [1; \boldsymbol{\xi}_{[T]}] \in A\right\}\right)$, $A \in \sigma(\Xi)$, Ξ is any closed convex set containing the support set of $\mathbb{P}$, Υ is the ambiguity set of $\mathbb{P}$. In this framework, we focus on finding binary functions $\boldsymbol{x}_t\left(\boldsymbol{\xi}_{[t_1]^\wedge}\right)$ and real-valued functions $\boldsymbol{y}_t\left(\boldsymbol{\xi}_{[t_2]^\wedge}\right)$ to solve the model.

Compared to (23), besides to continuous variables (dispatch decisions), the binary variables (unit status) in ours (24) also are modeled as functions of uncertain variables, which implies adaptivity and non-anticipativity in unit status since binary variables in t period only depend on uncertain variables in the previous periods without the later periods. Here, we provide a unified framework for typical DROs in the recent literature:

1) (23) is a special case of (24) when $t_1 = 0.\ t_2 = t$.

2) (22) is a special case of (24) when $t_1 = 0$ and $t_2 = T$.

3) when $t_1 \le t, t_2 = t$. It is the most important scene for our model, which can be used to implement rolling UUC for power system. In this scene, with uncertain wind power are observed at a given time and the operational dispatch ($\boldsymbol{y}(\cdot)$) are made immediately, quick-start units can be scheduled immediately ($t_1 = t$), slow-start units can be scheduled several time periods after the observation ($t_1 < t$).

Without loss of generality, for the convenience of discussion, this paper mainly discuss $t_1 = t_2 = t$, but everything discussed in this paper can be easily generalized to the general version of our framework (24).

B. Reformulation of the Proposed Model

[30] has shown that solving the class of problems (23) involving only single point set Υ and real-valued decisions is NP-hard in theory. In order to tract the more complex (24), in this subsection, we first use more flexibility *non-linear mixed decision rules* [25], to approximation restricts the infinite space of the adaptive decisions $\boldsymbol{x}_t(\cdot)$ and $\boldsymbol{y}_t(\cdot)$, which will gain back some degree of optimality while drastic simplifying computation. Second, we equivalently transform the DRO problem to MILP based on duality theory.

1) Data-driven uncertainty set

Given a set $\{\boldsymbol{P}^{\mathrm{W},j}\}_{j=1}^{M}$ of M samples. Then, $\bar{\boldsymbol{P}}^{\mathrm{W}} = \frac{1}{M}\sum_{j=1}^{M}\boldsymbol{P}^{\mathrm{W},j}$, $\boldsymbol{v}^{\mathrm{W},j} = \boldsymbol{P}^{\mathrm{W},j} - \bar{\boldsymbol{P}}^{\mathrm{W}}$, $\boldsymbol{\xi}^j \coloneqq [1; \boldsymbol{v}^{\mathrm{W},j}]$.

let $v_{i,t}^{\mathrm{w}-} = \min\{v_{i,t}^{\mathrm{w},j}, j = 1, \dots, M\}$, $v_{i,t}^{\mathrm{w}+} = \max\{v_{i,t}^{\mathrm{w},j}, j = 1, \dots, M\}$, $\boldsymbol{v}^{\mathrm{w}-} = \left[v_{[R],[T]}^{\mathrm{w}-}\right]^{\mathrm{T}}$, $\boldsymbol{v}^{\mathrm{w}+} = \left[v_{[R],[T]}^{\mathrm{w}+}\right]^{\mathrm{T}}$. Then, we have the data-driven support of $\mathbb{P}$, i.e.

$$\Xi = \left\{\boldsymbol{\xi}\middle|\boldsymbol{\xi}^- \coloneqq \begin{bmatrix}1\\ \boldsymbol{v}^{\mathrm{w}-}\end{bmatrix} \le \boldsymbol{\xi} \le \boldsymbol{\xi}^+ \coloneqq \begin{bmatrix}1\\ \boldsymbol{v}^{\mathrm{w}+}\end{bmatrix}\right\} \tag{25}$$

Unbiased moment estimator [26] is used to estimate $\widehat{\boldsymbol{\mu}}$ and $\widehat{\boldsymbol{\Sigma}}$:

$$\widehat{\boldsymbol{\mu}} = 0, \tag{26}$$

$$\widehat{\boldsymbol{\Sigma}} = \frac{1}{M}\sum_{j=1}^{M}\boldsymbol{\xi}^j(\boldsymbol{\xi}^j)^{\mathrm{T}}. \tag{27}$$

Where $\widehat{\boldsymbol{\mu}}$ is the mean matrix and $\widehat{\boldsymbol{\Sigma}}$ is a positive semi-definite covariance matrix, and is assumed as a positive definite matrix in the sequel, because in the case we study it always holds unless $\boldsymbol{\xi}^j = \widehat{\boldsymbol{\mu}}, \forall j = 1, \dots, M$).

2) Non-linear operator and lifted uncertainty set

We first insert $r_{i,t} - 1$ breakpoints into the marginal support of each uncertain variable $\xi_{i,t}$(include $\xi_{0,0}$, where $r_{0.0} = 1$) as follows:

$$v_{i,t}^{\mathrm{w}-} = p_{i,t}^0 < p_{i,t}^1 < \cdots < p_{i,t}^{r_{i,t}-1} < p_{i,t}^{r_{i,t}} = v_{i,t}^{\mathrm{w}+}. \tag{28}$$

Lifting operators $\bar{L}$ [25] and $\hat{L}$ [31] are introduced to facilitate the construction of flexible mixed decision rules:

$$\bar{\xi}_{i,t}^j = \bar{L}_{i,t}^j(\xi_{i,t}) \coloneqq \begin{cases} \xi_{i,t} & , \text{if } r_{i,t} = 1, j = 0 \\ \left\{\min\left\{\xi_{i,t}, p_{i,t}^j\right\} - p_{i,t}^{j-1}\right\}^+ & , \text{if } r_{i,t} > 1, j = 2, \dots, r_{i,t} \end{cases} \tag{29}$$

$$\hat{\xi}_{i,t}^j = \hat{L}_{i,t}^j(\xi_{i,t}) \coloneqq \begin{cases} 1 & \text{if } r_{i,t} = 1, j = 0 \\ \mathbb{1}\left(\xi_{i,t} \ge p_{i,t}^j\right) & \text{if } r_{i,t} > 1, j = 1, \dots, r_{i,t} - 1 \end{cases} \tag{30}$$

$$\bar{\xi}_{0,0} = \bar{L}_{0,0}(\xi_{0,0}) \coloneqq \bar{L}_{0,0}^0(\xi_{0,0}) = 1 \tag{31}$$

$$\hat{\xi}_{0,0} = \hat{L}_{0,0}(\xi_{0,0}) \coloneqq \hat{L}_{0,0}^0(\xi_{0,0}) = 1 \tag{32}$$

The lifting operator $\bar{L}_{i,t}$ converts the original uncertain variables $\xi_{i,t}$ into $\bar{\boldsymbol{\xi}}_{i,t} \coloneqq \left[\bar{\xi}_{i,t}^1; \dots; \bar{\xi}_{i,t}^{r_{i,t}}\right]$ which is a vector of lifted continuous parameters. The resulted continuous piecewise decision rule will provide better approximations than classical linear/affine decision rules. While lifting operator $\hat{L}_{i,t}$ converts $\xi_{i,t}$ to be a vector of lifted binary parameters $\hat{\boldsymbol{\xi}}_{i,t} \coloneqq \left[\hat{\xi}_{i,t}^1; \dots; \hat{\xi}_{i,t}^{r_{i,t}-1}\right]$.

Then we have the uncertainty set of $\tilde{\boldsymbol{\xi}}_{0,0}$, and $\tilde{\boldsymbol{\xi}}_{i,t}$:

$$\tilde{\Xi}_{0,0} \coloneqq \left\{\tilde{\boldsymbol{\xi}}_{0,0}\right\} \tag{33}$$

$$\tilde{\Xi}_{i,t} \coloneqq \left\{\tilde{\boldsymbol{\xi}}_{i,t}\middle|\xi_{i,t} \in \left[\xi_{i,t}^-, \xi_{i,t}^+\right], \bar{\boldsymbol{\xi}}_{i,t}, \hat{\boldsymbol{\xi}}_{i,t}\right\} \tag{34}$$

$\tilde{\boldsymbol{\xi}}$ is separable in each component $\tilde{\boldsymbol{\xi}}_{i,t}$ and $\tilde{\boldsymbol{\xi}}_{0,0}$, then, the uncertainty set of $\tilde{\boldsymbol{\xi}}$ is

$$\tilde{\Xi} \coloneqq \left\{\tilde{\boldsymbol{\xi}}\middle|\tilde{\boldsymbol{\xi}}_{0,0} \in \tilde{\Xi}_{0,0}, \tilde{\boldsymbol{\xi}}_{i,t} \in \tilde{\Xi}_{i,t}\right\} \tag{35}$$

$\tilde{\Xi}_{i,t}$ is an open set because of the discontinuity of $\hat{\boldsymbol{\xi}}_{i,t}$. Then, we're going to give the closed convex hull of $\tilde{\Xi}_{i,t}$ denote as $\mathrm{conv}\left(\mathrm{cl}\left(\tilde{\Xi}_{i,t}\right)\right)$ [20], [31] to further reformulation. Firstly, the sets of vertices in $\tilde{\Xi}_{i,t}$ and $\tilde{\Xi}_{0,0}$ are defined:

$$\tilde{\mathcal{V}}_{i,t} = \bigcup_{j=1}^{r_{i,t}} \tilde{\mathcal{V}}_{i,t}^j \tag{36}$$

$$\tilde{\mathcal{V}}_{i,t}^j = \left\{\tilde{\boldsymbol{v}}_{i,t} = \left[v_{i,t}; \bar{\boldsymbol{v}}_{i,t}; \hat{\boldsymbol{v}}_{i,t}\right]\middle|\begin{matrix} v_{i,t} \in \left\{p_{i,t}^{j-1}, p_{i,t}^j\right\} \\ \bar{\boldsymbol{v}}_{i,t} = \bar{L}_{i,t}(v_{i,t}) \\ \hat{\boldsymbol{v}}_{i,t} = \lim\limits_{\xi_{i,t} \to v_{i,t}, \xi_{i,t} \in \left[p_{i,t}^{j-1}, p_{i,t}^j\right]} \hat{L}_{i,t}(\xi_{i,t}) \end{matrix}\right\} \forall j \in [r_{i,t}] \tag{37}$$

$$\tilde{\mathcal{V}}_{0,0} = \{[1; 1; 1]\} \tag{38}$$

Then, $\mathrm{conv}\left(\mathrm{cl}\left(\tilde{\Xi}_{i,t}\right)\right)$ can be formulated as:

$$\mathrm{conv}\left(\mathrm{cl}\left(\tilde{\Xi}_{i,t}\right)\right) = \left\{\tilde{\boldsymbol{\xi}}_{i,t}\middle|\begin{matrix} \sum_{\tilde{v}_{i,t} \in \tilde{\mathcal{V}}_{i,t}^j} \lambda_{i,t}\left(\tilde{v}_{i,t}\right) = 1 \\ \tilde{\boldsymbol{\xi}}_{i,t} = \sum_{\tilde{v}_{i,t} \in \tilde{\mathcal{V}}_{i,t}^j} \lambda_{i,t}\left(\tilde{\boldsymbol{v}}_{i,t}\right)\tilde{\boldsymbol{v}}_{i,t} \\ \xi_{i,t} \in \left[\xi_{i,t}^-, \xi_{i,t}^+\right] \\ \lambda_{i,t}\left(\tilde{\boldsymbol{v}}_{i,t}\right) \in \Re_+, \forall \tilde{\boldsymbol{v}}_{i,t} \in \tilde{\mathcal{V}}_{i,t} \end{matrix}\right\} \tag{39}$$

where $\lambda_{i,t}\left(\tilde{v}_{i,t}\right)$ is the coefficient associated with vertex $\tilde{v}_{i,t} \in \tilde{\mathcal{V}}_{i,t}$.

$$\mathrm{conv}\left(\mathrm{cl}\left(\tilde{\Xi}_{0,0}\right)\right) = \{[1; 1; 1]\} \tag{40}$$

It can be seen from (33)(34)(35) that $\tilde{\Xi}$ is separable in each component $\tilde{\boldsymbol{\xi}}_{i,t}$ and $\tilde{\boldsymbol{\xi}}_{0,0}$. Therefore, we have

$$\mathrm{conv}\left(\mathrm{cl}\left(\tilde{\Xi}_S\right)\right) = \left\{\tilde{\boldsymbol{\xi}}\middle|\tilde{\boldsymbol{\xi}}_{i,t} \in \mathrm{conv}\left(\mathrm{cl}\left(\tilde{\Xi}_{i,t}\right)\right), \forall (i,t) \in S\right\} \tag{41}$$

where $S \subseteq \{(0,0), (1,1), \dots, (i,t), \dots, (R,T)\}$.

3) Data-Driven Lifted ambiguity set

On the basis of uncertainty set, we construct the ambiguity set based on Wasserstein-metric through prior knowledge or historical data, which can provide a flexible framework for decision maker to model uncertainty through partial information. The Wasserstein-metric is defined as:

$$W(\mathbb{Q}, \mathbb{P}) = \inf_{\pi \in m(\hat{\Xi} \times \hat{\Xi})}\{\mathbb{E}_\pi[d(\xi^q, \xi^p)]: \xi^q \sim \mathbb{Q}, \xi^p \sim \mathbb{P}\} = \inf_{\pi \in m(\hat{\Xi} \times \hat{\Xi})}\left\{\int_{\hat{\Xi} \times \hat{\Xi}} d(\xi^q, \xi^p)\pi(\mathrm{d}\xi^q, \mathrm{d}\xi^p): \pi\left(\hat{\Xi}, \mathrm{d}\xi^p\right) = \mathbb{P}(\mathrm{d}\xi^p), \pi\left(\mathrm{d}\xi^q, \hat{\Xi}\right) = \mathbb{Q}(\mathrm{d}\xi^q)\right\} \tag{42}$$

$$d(\xi^q, \xi^p) = \|\xi^q - \xi^p\| \tag{43}$$

Where $\hat{\Xi}$ is a compact supporting space and $\mathbb{P}$, $\mathbb{Q}$ are two probability distribution in $\hat{\Xi}$. $m(\cdot)$ is the set of probability measures on a measurable space $(\cdot, \mathcal{F})$, the distance between uncertain variables ξ^q and ξ^p is defined by $d(\xi^q, \xi^p)$, ξ^q and

ξ^p are follow distribution $\mathbb{Q}$ and $\mathbb{P}$, respectively, and the infimum is taken over all joint distributions π with marginals $\mathbb{Q}$ and $\mathbb{P}$.

Given the lifted uncertain parameters $\tilde{\boldsymbol{\xi}}$ with supporting space $\mathrm{conv}\left(\mathrm{cl}\left(\tilde{\Xi}\right)\right)$, the Wasserstein-metric on ambiguity set Υ can be expressed as [17]:

$$\mathbb{B}_\varepsilon\left(\widetilde{\mathbb{P}}_M\right)=\left\{\widetilde{\mathbb{Q}}\middle|W\left(\widetilde{\mathbb{Q}},\widetilde{\mathbb{P}}_M\right)\le\varepsilon\right\} \tag{44}$$

A sample j in the lifted space is $\tilde{\boldsymbol{\xi}}^j=L(\boldsymbol{\xi}^j:=[1;\boldsymbol{P}^{\mathrm{w},j}])$, and the empirical distribution with M samples can be expressed as

$$\widetilde{\mathbb{P}}_M=\frac{1}{M}\sum_{j=1}^{M}\delta_{\tilde{\xi}^j} \tag{45}$$

where $\delta_{\tilde{\xi}^j}$ is a Dirac measure.

Intuitively, as $M\to\infty$, $\widetilde{\mathbb{P}}_M$ should tend to the true distribution $\widetilde{\mathbb{P}}^*$ of $\tilde{\boldsymbol{\xi}}$.

Parameter ε plays an important role in the performance of ambiguity set, which can weight the robustness and economy. Meanwhile, it can be calculated by statistical methods, such as the one given in reference [16]:

$$P\{W(\mathbb{Q},\mathbb{P})\le\varepsilon\}\ge 1-\exp\left(-M\frac{\varepsilon^2}{C^2}\right) \tag{46}$$

$$\varepsilon=C\sqrt{\frac{1}{M}\ln\left(\frac{1}{1-\eta}\right)} \tag{47}$$

Where η is the given confidence level and C is a constant which can be approximately obtained by solving the following problem:

$$C\approx\min_{\rho>0}2\sqrt{\frac{1}{2\rho}\left(1+\ln\left(\frac{1}{M}\sum_{j=1}^{M}e^{\rho\left\|\tilde{\xi}^j-\tilde{\mu}\right\|_1^2}\right)\right)} \tag{48}$$

where $\tilde{\mu}=\frac{1}{M}\sum_{j=1}^{M}\tilde{\boldsymbol{\xi}}^j$.

4) Mixed decision rules

We adopt mixed decision rules to restrict uncertain variables to be linear functions of the lifted parameters:

$$\boldsymbol{x}_t\left(\boldsymbol{\xi}_{[t]^\wedge}\right)=\hat{X}^t_{[t]^\wedge}\hat{\boldsymbol{\xi}}_{[t]^\wedge},\forall t\in[T] \tag{49}$$

$$\boldsymbol{y}_t\left(\boldsymbol{\xi}_{[t]^\wedge}\right)=\bar{Y}^t_{[t]^\wedge}\bar{\boldsymbol{\xi}}_{[t]^\wedge},\forall t\in[T] \tag{50}$$

Compared with classical decision rules that only model continuous variables [27], the mixed decision rules of Eq. (49) and (50) further consider binary variables while maintaining linearity. Furthermore, the decision rule (50) grants continuous variables to follow commonly piecewise linear functions, which is essential in mixed integer problems.

It can be seen that, with the given domain for $\hat{X}^t_{[t]^\wedge}$, the decision rules (49) are guaranteed to generate binary decision variable $\boldsymbol{x}_t$ even if the associated constraints are relaxed to $\boldsymbol{0}\le\boldsymbol{x}_t\left(\boldsymbol{\xi}_{[t]^\wedge}\right)\le\boldsymbol{e}$ [31]. In next subsection, we address the linear inequality constraints of $(24)^2$.

5) Reformulation of inequality constraints

First, decision rules (49) (50) are substituted into $(24)^2$, then the lifted uncertainty set $\mathrm{conv}\left(\mathrm{cl}\left(\tilde{\Xi}_{S^t}\right)\right)$ is introduced, and constraints $(24)^2$ can be reformulated as:

$$\sum_{\tau=1}^{t}\left[\boldsymbol{B}^t_\tau\bar{Y}^\tau_{[\tau]^\wedge}\bar{\boldsymbol{\xi}}_{[\tau]^\wedge}+\boldsymbol{A}^t_\tau\hat{X}^\tau_{[\tau]^\wedge}\hat{\boldsymbol{\xi}}_{[\tau]^\wedge}\right]\le\boldsymbol{D}^t\boldsymbol{\xi}_{[t]^\wedge},\forall t\in[T] \tag{51}$$

where $S^t=\{(i,\tau)|i\in[R],\tau\in[t]\}\cup\{(0,0)\}$, $\forall\vec{\tilde{\boldsymbol{\xi}}}_{[t]^\wedge}\in\mathrm{conv}\left(\mathrm{cl}\left(\tilde{\Xi}_{S^t}\right)\right)$, all of these conditions are met below and will not be described further.

Let $\vec{\tilde{\boldsymbol{\xi}}}_{[t]^\wedge}=\left[\boldsymbol{\xi}_{[t]^\wedge};\bar{\boldsymbol{\xi}}_{[\tau]^\wedge};\hat{\boldsymbol{\xi}}_{[\tau]^\wedge}\right]$, we rewrite $\mathrm{conv}\left(\mathrm{cl}\left(\tilde{\Xi}_{S^t}\right)\right)$ to be:

$$\mathrm{conv}\left(\mathrm{cl}\left(\tilde{\Xi}_{S^t}\right)\right)=\left\{\vec{\tilde{\boldsymbol{\xi}}}_{[t]^\wedge}\middle|\begin{matrix}\boldsymbol{W}^1_{[t]^\wedge}\vec{\tilde{\boldsymbol{\xi}}}_{[t]^\wedge}+\boldsymbol{U}^1_{[t]^\wedge}\vec{\boldsymbol{\lambda}}_{[t]^\wedge}\ge\boldsymbol{h}^1_{[t]^\wedge}\\ \boldsymbol{W}^2_{[t]^\wedge}\vec{\tilde{\boldsymbol{\xi}}}_{[t]^\wedge}+\boldsymbol{U}^2_{[t]^\wedge}\vec{\boldsymbol{\lambda}}_{[t]^\wedge}=\boldsymbol{h}^2_{[t]^\wedge}\end{matrix}\right\} \tag{52}$$

(51) can be rewritten as:

$$Z^t_{[t]^\wedge}\vec{\tilde{\boldsymbol{\xi}}}_{[t]^\wedge}\ge 0,\forall t\in[T] \tag{53}$$

Where

$Z^t_{[t]^\wedge}=[-\boldsymbol{D}^t\quad\mathfrak{B}^t\quad\mathfrak{A}^t]$

$\mathfrak{B}^t=\left[\boldsymbol{B}^t_{[t]}\bar{Y}^{[t]}_0\quad\boldsymbol{B}^t_{[1:t]}\bar{Y}^{[1:t]}_1\quad\boldsymbol{B}^t_{[2:t]}\bar{Y}^{[2:t]}_2\quad\dots\quad\boldsymbol{B}^t_{[t:t]}\bar{Y}^{[t:t]}_t\right]$

$\mathfrak{A}^t=\left[\boldsymbol{A}^t_{[t]}\hat{X}^{[t]}_0\quad\boldsymbol{A}^t_{[1:t]}\hat{X}^{[1:t]}_1\quad\boldsymbol{A}^t_{[2:t]}\hat{X}^{[2:t]}_2\quad\dots\quad\boldsymbol{A}^t_{[t:t]}\hat{X}^{[t:t]}_t\right]$

By applying standard robust counterpart reformulation techniques (Proposition 4 in [31]), (53) can be reconstructed as the following set of constraints:

$$\begin{cases}\Lambda^k_{[t]^\wedge}\boldsymbol{W}^k_{[t]^\wedge}=Z^k_{[t]^\wedge}\\ \left(\boldsymbol{U}^k_{[t]^\wedge}\right)^{\mathrm{T}}\Lambda^k_{[t]^\wedge}=0\\ \left(\boldsymbol{h}^k_{[t]^\wedge}\right)^{\mathrm{T}}\Lambda^k_{[t]^\wedge}\ge 0\\ \Lambda^1_{[t]^\wedge}\ge 0\end{cases}\forall t\in[T],k=1,2 \tag{54}$$

6) Reformulation of equality constraints

Similarly, constraints $(24)^3$ can be re-expressed as follows:

$$\sum_{\tau=1}^{t}\left[\boldsymbol{\mathcal{B}}^t_\tau\bar{Y}^\tau_{[\tau]^\wedge}\bar{\boldsymbol{\xi}}_{[\tau]^\wedge}+\boldsymbol{\mathcal{A}}^t_\tau\hat{X}^\tau_{[\tau]^\wedge}\hat{\boldsymbol{\xi}}_{[\tau]^\wedge}\right]=\boldsymbol{d}^t,\forall t\in[T] \tag{55}$$

(55) can be rewritten as

$$\mathcal{Z}^t_{[t]^\wedge}\vec{\tilde{\boldsymbol{\xi}}}_{[t]^\wedge}=\boldsymbol{d}^t,\forall t\in[T] \tag{56}$$

Where $\mathcal{Z}^t_{[t]^\wedge}$ and $Z^t_{[t]^\wedge}$ are arranged in the same way.

$$\mathcal{Z}^{t,j}_{[t]^\wedge}\vec{\tilde{\boldsymbol{\xi}}}_{[t]^\wedge}=\boldsymbol{d}^{t,j},\forall t\in[T] \tag{57}$$

$\mathcal{Z}^{t,j}_{[t]^\wedge}$, and $\boldsymbol{d}^{t,j}$ are the jth rows of $\mathcal{Z}^t_{[t]^\wedge}$ and $\boldsymbol{d}^t$ respectively.

For any $\tilde{\mathcal{V}}_{i,t}$, it is not very hard to verify that all the points in this set are linearly independent. The dimension of $\tilde{\mathcal{V}}_{i,t}$ is $2r_{i,t}$ and $\left|\tilde{\mathcal{V}}_{i,t}\right|=2r_{i,t}$. Taking the separability of $\mathrm{conv}\left(\mathrm{cl}\left(\tilde{\Xi}_{S^t}\right)\right)$, we can construct $\mathcal{r}=\sum_{(i,t)\in S^t}2r_{i,t}$ linearly independent vectors $(\vec{\tilde{\boldsymbol{\xi}}}^k_{[t]^\wedge},k\in[\mathcal{r}])$ which belong to $\mathrm{conv}\left(\mathrm{cl}\left(\tilde{\Xi}_{S^t}\right)\right)$.

Then (57) imply that

$$\mathcal{Z}^{t,j}_0\boldsymbol{e}+\mathcal{Z}^{t,j}_{[t]}\vec{\tilde{\boldsymbol{\xi}}}^k_{[t]}=\boldsymbol{d}^{t,j},\forall k\in[\mathcal{r}],\forall t\in[T] \tag{58}$$

Then, we have that

$\mathcal{Z}^{t,j}_0\boldsymbol{e}=\boldsymbol{d}^{t,j}$

$\mathcal{Z}^{t,j}_{[t]}=\boldsymbol{0}$

Then, (56) is equivalent to

$\mathcal{Z}^t_0\boldsymbol{e}=\boldsymbol{d}^t$

$\mathcal{Z}^t_{[t]}=\boldsymbol{0}$

7) Reformulation of DR objective function

Let $\ell\left(\vec{\tilde{\boldsymbol{\xi}}}\right)=\sum_{t=1}^{T}\left[\boldsymbol{c}_t^{\mathrm{T}}\boldsymbol{x}_t\left(\boldsymbol{\xi}_{[t]^\wedge}\right)+\boldsymbol{d}_t^{\mathrm{T}}\boldsymbol{y}_t\left(\boldsymbol{\xi}_{[t]^\wedge}\right)\right]=c^{\mathrm{T}}\vec{\tilde{\boldsymbol{\xi}}}$, where c^{T} and $Z^t_{[t]^\wedge}$ are arranged in the same way.

The objective function is ambitious to be reformulated because it is an optimization problem to guarantee worst-case expectation on ambiguity set. Fortunately, [17] developed the

strong duality theory gives the reformulation of the worst-case expectation, i.e., the inner of (24) can be rewritten as:

$$\min_{\lambda_j,\beta\geq 0} \sum_{j=1}^{M} \lambda_j + \varepsilon\beta \tag{59}$$

$$\text{s.t.}\left\{\ell\left(\vec{\tilde{\xi}}\right) - M\lambda_j - \beta d\left(\vec{\tilde{\xi}}, \vec{\tilde{\xi}}^{\,j}\right) \leq 0, , \forall j = 1 \ldots, M\right.$$

Let $\tilde{\lambda}_j = M\lambda_j$, the constraints in (59) can be written as follows:

$$\sup_{\vec{\tilde{\xi}}\in \mathrm{conv}\left(\mathrm{cl}\left(\Xi_{St}\right)\right)} \left\{\ell\left(\vec{\tilde{\xi}}\right) - \beta d\left(\vec{\tilde{\xi}}, \vec{\tilde{\xi}}^{\,j}\right)\right\} \leq \tilde{\lambda}_j, \forall j = 1 \ldots, M \tag{60}$$

Lemma 1: $\omega d(\boldsymbol{\lambda}, \boldsymbol{\lambda}^j) = \sup_{\|\boldsymbol{p}\|_*\leq\omega} \langle p, \boldsymbol{\lambda} - \boldsymbol{\lambda}^j\rangle$.

$$-\beta d\left(\vec{\tilde{\xi}}, \vec{\tilde{\xi}}^{\,j}\right) = -\sup_{\|\tilde{\boldsymbol{p}}^j\|_*\leq\beta} \langle \tilde{\boldsymbol{p}}^j, \vec{\tilde{\xi}} - \vec{\tilde{\xi}}^{\,j}\rangle = \inf_{\|\tilde{\boldsymbol{p}}^j\|_*\leq\beta} \langle \tilde{\boldsymbol{p}}^j, \vec{\tilde{\xi}}^{\,j} - \vec{\tilde{\xi}}\rangle \tag{61}$$

Then, by substituting (61) and mixed decision rules (49) and (50) into (60), and interchanging the outer maximization over $\tilde{\boldsymbol{\xi}}$ and the infimum over $\tilde{\boldsymbol{p}}^j$, which is allowed by the minimax theorem, we obtain the following reformulation of (60):

$$\sup_{\vec{\tilde{\xi}}\in \mathrm{conv}\left(\mathrm{cl}\left(\Xi_{St}\right)\right)} \left\{c^{\mathrm{T}}\vec{\tilde{\xi}} + \inf_{\|\tilde{\boldsymbol{p}}^j\|_*\leq\beta} \langle \tilde{\boldsymbol{p}}^j, \vec{\tilde{\xi}}^{\,j} - \vec{\tilde{\xi}}\rangle\right\}$$

$$= \inf_{\|\tilde{\boldsymbol{p}}^j\|_*\leq\beta} \left\{\langle \tilde{\boldsymbol{p}}^j, \vec{\tilde{\xi}}^{\,j}\rangle + S_{\mathrm{conv}\left(\mathrm{cl}\left(\Xi_{St}\right)\right)}(c^{\mathrm{T}} - \tilde{\boldsymbol{p}}^j)\right\} \tag{62}$$

$$S_{\mathrm{conv}\left(\mathrm{cl}\left(\Xi_{St}\right)\right)}(c^{\mathrm{T}} - \tilde{\boldsymbol{p}}^j) = \sup_{\vec{\tilde{\xi}}\in \mathrm{conv}\left(\mathrm{cl}\left(\Xi_{St}\right)\right)} \langle c^{\mathrm{T}} - \tilde{\boldsymbol{p}}^j, \vec{\tilde{\xi}}\rangle =$$

$$\inf_{\boldsymbol{y}_j}\left\{\langle \boldsymbol{h}, \boldsymbol{y}_j\rangle : [\boldsymbol{W}^{\mathrm{T}}; \boldsymbol{U}^{\mathrm{T}}]\boldsymbol{y}_j = [c^{\mathrm{T}} - \tilde{\boldsymbol{p}}^j; 0], \boldsymbol{y}_j \leq 0\right\} \tag{63}$$

According to (63), we have

$$\tilde{\boldsymbol{p}}^j = c^{\mathrm{T}} - \boldsymbol{W}^{\mathrm{T}}\boldsymbol{y}_j \tag{64}$$

According to (60)(62), the (59) is equivalent to

$$\min_{\lambda_j,\beta\geq 0,\tilde{\boldsymbol{p}}^j} \sum_{j=1}^{M} \lambda_j + \varepsilon\beta \tag{65}$$

$$\text{s.t.}\begin{cases}\langle \tilde{\boldsymbol{p}}^j, \vec{\tilde{\xi}}^{\,j}\rangle + S_{\mathrm{conv}\left(\mathrm{cl}\left(\Xi_{St}\right)\right)}(c^{\mathrm{T}} - \tilde{\boldsymbol{p}}^j) \leq \tilde{\lambda}_j \\ \left\|\tilde{\boldsymbol{p}}^j\right\|_* \leq \beta\end{cases} \forall j = 1 \ldots, M$$

According to (63)(64), the (65) is equivalent to

$$\min_{\lambda_j,\beta\geq 0,\boldsymbol{y}_j\geq 0} \sum_{j=1}^{M} \lambda_j + \varepsilon\beta \tag{66}$$

$$\text{s.t.}\begin{cases}\langle c^{\mathrm{T}} - \boldsymbol{W}^{\mathrm{T}}\boldsymbol{y}_j, \vec{\tilde{\xi}}^{\,j}\rangle + \langle \boldsymbol{h}, \boldsymbol{y}_j\rangle \leq \tilde{\lambda}_j \\ \left\|c^{\mathrm{T}} - \boldsymbol{W}^{\mathrm{T}}\boldsymbol{y}_j\right\|_* \leq \beta \\ \boldsymbol{U}^{\mathrm{T}}\boldsymbol{y}_j = 0\end{cases} \forall j = 1 \ldots, M$$

C. Resulted DR-MDR Model

$$\min_{\lambda_j,\beta\geq 0,\boldsymbol{y}_j\geq 0,\Lambda_{[t]^\wedge}\geq 0} \sum_{j=1}^{M} \lambda_j + \varepsilon\beta \tag{67}$$

$$\text{s.t.}\begin{cases}\langle c^{\mathrm{T}} - \boldsymbol{W}^{\mathrm{T}}\boldsymbol{y}_j, \vec{\tilde{\xi}}^{\,j}\rangle + \langle \boldsymbol{h}, \boldsymbol{y}_j\rangle \leq \tilde{\lambda}_j \\ \left\|c^{\mathrm{T}} - \boldsymbol{W}^{\mathrm{T}}\boldsymbol{y}_j\right\|_* \leq \beta \\ \boldsymbol{U}^{\mathrm{T}}\boldsymbol{y}_j = 0 \\ \Lambda_{[t]^\wedge}\boldsymbol{W}_{[t]^\wedge} = Z_{[t]^\wedge} \\ \boldsymbol{U}_{[t]^\wedge}^{\mathrm{T}}\Lambda_{[t]^\wedge} = 0 \\ \boldsymbol{h}_{[t]^\wedge}^{\mathrm{T}}\Lambda_{[t]^\wedge} \geq 0 \\ \mathcal{Z}_0^t\boldsymbol{e} = \boldsymbol{d}^t \\ \mathcal{Z}_{[t]}^t = \boldsymbol{0}\end{cases} \forall t \in [T], \forall j = [M]$$

IV. Numerical Results and Analysis

A. Simulation Setup

In this paper, select IEEE 6-bus and 30-bus test system for simulations to authenticate the advantages and superiority of our model. The simulations are conducted on a laptop with Intel Core i5-4200M CPU@2.60GHz and 8GB RAM running Windows 10 operating system. Commercial solver MOSEK and CPLEX from Yalmip are used to solve the model. The thermal unit parameters of 6-bus system are given in Table I, for the sake of brevity, data of 30-bus system are not listed here [32]. All of the codes and cases for this paper are available for free download on GitHub [33]. And we used one year's historical wind data as samples, the samples set divided by monthly data, i.e., every 30 groups of daily historical wind data we taken as a sample set. Specially, Fig. 3. Shows the wind power in a sample set (30-samples). X-axis represents a scheduling periods of 24 hours a day, Z-axis represents the samples in the current group, every 5 samples are represented by a color, and Y-axis represents the specific wind power of the corresponding samples in the corresponding period. It is not difficult to see from Fig. 3. That the more severe the curve fluctuation is, the more unstable the wind power in this group of samples is, and the more difficult the model to adapt to such a complex scenario. For example, the wind power of Sample 30 is obviously more unstable than that of Sample 28. In this chapter, we will use multiple sample sets to conduct simulation experiments to verify that the proposed model outperforms traditional model in various scenario.

TABLE I
Thermal unit parameters of 6-bus test system

Bus No.	$\bar{P}_i^{\mathrm{G}}$[MW]	$\underline{P}_i^{\mathrm{G}}$[MW]	Cost coefficients		
			a[$/$h$]	b[$/MW h]	c[$/MW$h^2$]
1	200	50	0.00	2.00	0.00375
2	80	20	0.00	1.75	0.01750
6	50	15	0.00	1.00	0.06250
Bus No.	$P_{up,i}$	$P_{\mathrm{start},i}$	$P_{\mathrm{shut},i}$	$C_{hot,i}$	$C_{cold,i}$
1	55	110	220	0.1	0.2
2	50	50	100	2.00	4.00
6	20	10	20	1.00	2.00
Bus No.	$\underline{T}_{\mathrm{on},i}$	$\underline{T}_{\mathrm{off},i}$	$T_{\mathrm{cold},i}$		
1	4	4	4		
2	3	3	3		
6	1	0	1		

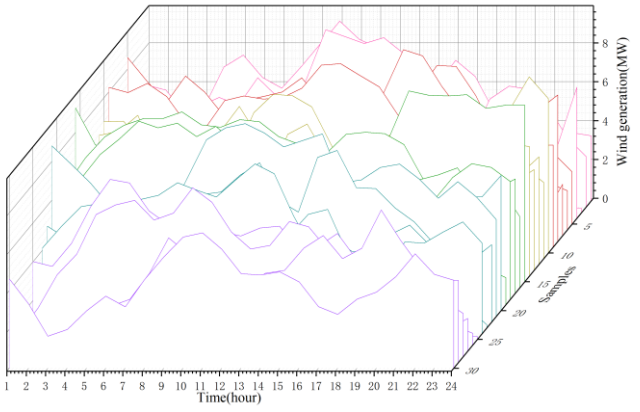

Fig. 3. Waterfall diagram of wind historical data

B. *Comparison with typical model*

For the sake of displaying the results, the control experiment was carried out based on a 6 bus-12 periods test system in this subsection. Fig. 4 Shows the total cost curve of our fully adaptive multi-stage distributionally robust model based on Wasserstein-metric and mixed decision rules (DR-MDR, Eq. (24)) and the typical multi-stage distributionally robust model (DR-TPMS, Eq. (22) and (23) refer to [13], [18], [19]) in different ambiguity set (the larger the ε is, the larger the ambiguity set is and the more robust model is) and different sample sets. Different sample sets (SPLs) were marked by different colors, and cost curve of DR-MDR and DR-TPMS were marked by lines and dotted lines respectively. Since the scheduling scheme obtained is applicable to any wind power in the ambiguity set, after obtaining the coefficients of integral $\hat{X}^{t}_{[t]^{\wedge}}$ and continuous $\hat{Y}^{t}_{[t]^{\wedge}}$ decision rules, a wind power $\boldsymbol{\xi}_{[t]^{\wedge}}$ is put into Eq. (49) and (50) (for example, unit state $u_{[G],t}\left(\boldsymbol{\xi}_{[t]^{\wedge}}\right) = \hat{X}^{[G],t}_{[t]^{\wedge}}\hat{\boldsymbol{\xi}}_{[t]^{\wedge}}$) to obtain all decision variables (the 18th samples in the sample set is selected in this subsection), different decision variables can be obtained for different wind power, then Eq. (8) can be used to calculate the generation cost. DR-TPMS is consistent except that there is no integer decision variable coefficient. Unit output comparison and wind generation comparison between DR-MDR and DR-TPMS in sample 3 with fixed $\varepsilon = 2.25$ is shown in Fig. 5 and Fig. 6 respectively. And Fig. 7 shows the three dimensions histogram of load loss comparison of DR-MDR and DR-TPMS in this case. X-axis represents time period, Y-axis represents current model and node, and Z-axis represents the load loss.

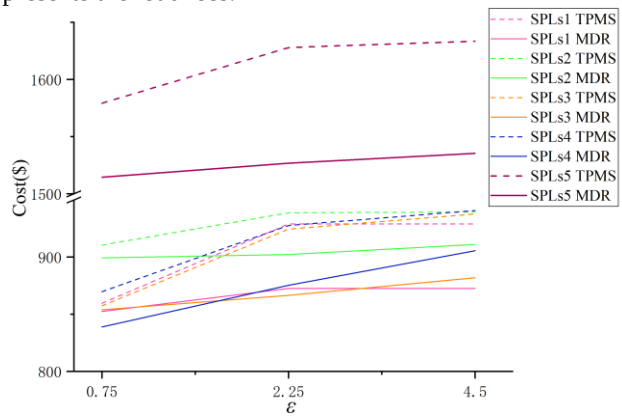

Fig. 4. System total cost comparison chart

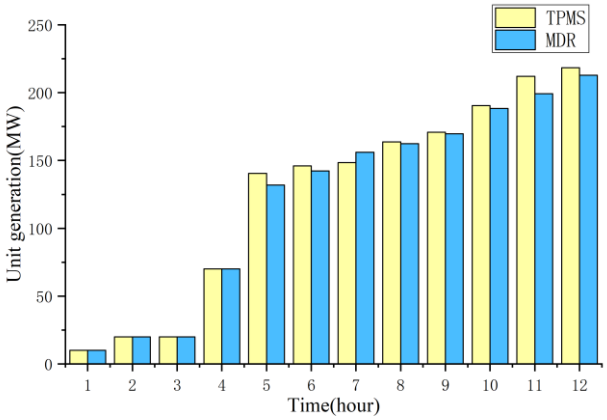

Fig. 5. Unit output comparison diagram

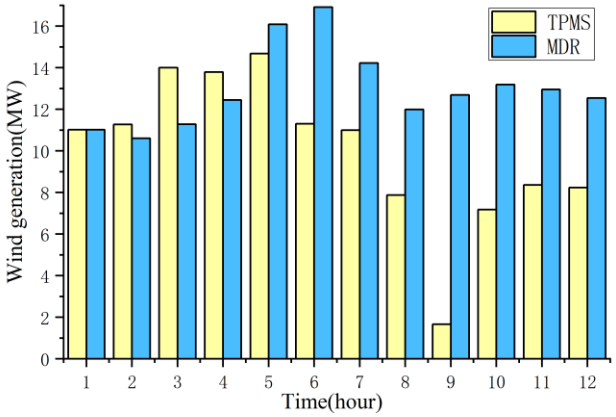

Fig. 6. Wind generation comparison diagram

Firstly, as show in Fig. 4, the total cost of DR-MDR is less its of DR-TPMS in any sample set, such conclusion is the same as the 1-1 system sample and the theoretical derivation of Eq. (23) and (24). Because DR-MDR, compared to DR-TPMS, increases the processing of integer decision variables and thus expands the feasible region, it is possible to find a better solution, i.e. a scheduling scheme with lower generation costs. Meanwhile, clearly when the wind fluctuation is larger (sample 5), the difference in generation cost between DR-MDR and DR-TPMS also increases significantly, which means that DR-MDR has a more obvious advantage than DR-TPMS in the case of unstable wind in the actual environment. In terms of ambiguity, the generation costs of both DR-MDR and DR-TPMS increase with the increase of ε. Then in theory, DR-TPMS fixes the on/off state of units, therefore, DR-MDR makes more reasonable use of wind power to reduce the output of units, this is consistent with the results in Fig. 5 and Fig. 6, that is, DR-MDR wind generation is more than DR-TPMS while thermal generation is less than DR-TPMS in most periods. Take period 6 as an example, as can be seen from Fig. 3, the wind power fluctuates greatly at this time (i.e., the variance is large, the waterfall drop of each sample is large in Fig. 3), which results in DR-MDR using more wind power generation than DR-TPMS, correspondingly, the total thermal generation of DR-MDR also decreases in this period. However, in such a small-period test system, the state of DR-MDR and DR-TPMS are the same, because when the test system has a small number of periods, in order to meet the load requirements, the unit state scheduling is basically on as far as possible, and the state scheduling scheme with a large number of periods may be different. It will better reflect the advantages of DR-MDR, which will be verified by a 24-period test system in the next subsection.

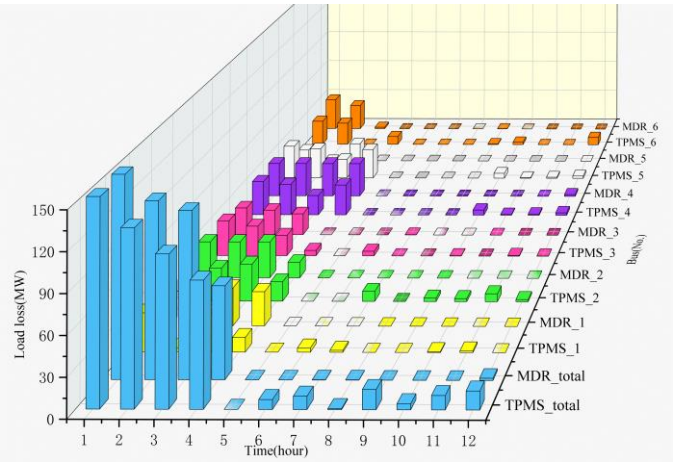

Fig. 7. Three dimensions histogram of load loss comparison

Finally, it can be seen from Fig. 6 and Fig. 7 that DR-MDR also reduces the load loss of each node in mostly period because it makes more use of wind power generation. Combined with Table I, we can find since thermal units is not fully started in the first four periods, there is no significant difference of DR-MDR and DR-TPMS. However, with the change of time, there is more scheduling space after the thermal units started, and the difference of the corresponding load loss of the two models is more obvious. At the same time, the reduction of load loss not only reduces the total power generation cost of DR-MDR scheduling scheme, but also meets the load requirements better than DR-TPMS while controlling the power generation cost from the perspective of user load.

C. Results on other IEEE test system

Previous experiments on 1-1 system and 6-12 system verified that the proposed model could better adapt to wind power compared to the typical multi-stage model. In this sub-section, we will conduct simulations on larger test system to verify that the advantages of DR-MDR are more significant based on larger system and longer period.

Theoretically, the larger the system scale, the longer the scheduling period, the larger the feasible region of DR-MDR, the more likely it is to find a better solution due to the application of MDR. However, as period increase the number of integer variables coefficient $\hat{X}^{t}_{[t]^{\wedge}}$ and continuous variables coefficient $\hat{Y}^{t}_{[t]^{\wedge}}$ will boost. Take t period increase to 2t period as an example, the numbers of variables coefficient of t period $N_t = (t + (t-1) + \cdots 1) \times (1 + bpN + bp)$ while the numbers of variables coefficient of 2t period $N_{2t} = (2t + (2t-1) + \cdots + t + (t-1) + \cdots 1) \times (1 + bpN + bp)$, N_{2t} is about $1.29 \times e^{15}$ times as great as N_t when $\mathrm{t} = 12$. In this case, clearly the high computational cost is not conductive to simulation. Therefore, we will choose 12 hours as scheduling period on 30-bus system. Fig. 8 shows the total cost comparison between DR-MDR and DR-TPMS on 6-12, 6-24 and 30-12 test system with fixed $\varepsilon = 2.25$. At the same time, in order to verify that DR-MDR can generate different on/off unit state scheduling schemes compared with DR-TPMS, we selected 6-24 system for simulation and put multiple wind power data and coefficient $\hat{X}^{t}_{[t]^{\wedge}}$ into (49) to obtain multiple different on/off unit state scheduling schemes $\left[u_{[G],1}, u_{[G],2} \ldots u_{[G],t}\right]^1$, $\left[u_{[G],1}, u_{[G],2} \ldots u_{[G],t}\right]^2, \ldots \ldots, \left[u_{[G],1}, u_{[G],2} \ldots u_{[G],t}\right]^n$, and the results are shown in Fig. 9. The abscissa represents period, the ordinate represents the on/off state of the unit, and 1 represents on and 0 represents off.

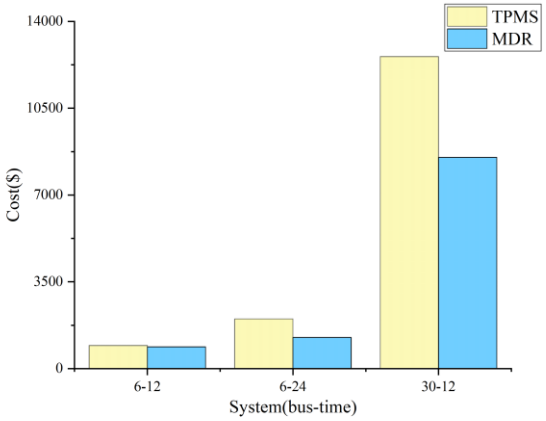

Fig. 8. Large-scale system total cost comparison diagram

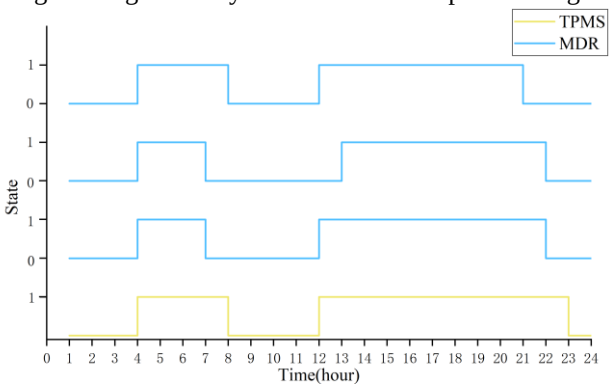

Fig. 9. Unit 1 statement diagram

It can be seen from Fig. 9 that since the on/off state of unit was determined before the scheduling of DR-TPMS, the line chart of the on/off state of DR-TPMS does not change with different wind power data. Therefore, there is only one yellow curve representing the on/off state of the DR-TPMS in Fig. 9. However, the on/off state scheduling scheme obtained by DR-MDR is an affine function of wind power, thus, when different wind power situations occur in the actual scenario, the scheduling scheme may also be different. As shown in Fig. 9, there are three different blue curves representing DR-MDR. It is not difficult to see that the scheduling scheme with different on/off state scheduling for different wind power can make better use of wind power. Then, it can be found from Fig. 8 that when the system is small (6-12), the system total costs of DR-MDR and DR-TPMS are very similar. However, as the system scale or the number of periods increases, the amount of wind power that can be used for optimization increases dramatically, and the difference in total costs between DR-MDR and DR-TPMS increases. The results from the two case studies are consistent with our theoretical derivation given in Section III.

V. Conclusion

We proposed a fully adaptive distributionally robust multi-stage uncertain unit commitment framework in this paper. Our model provides a unifying framework for several existing

DRO models, various typical models can be obtained by adjusting decision rules and relevant periods. Therefore, in the scenario where the existing model is not feasible, our model can usually find a feasible solution, and in the scenario where the existing model has a solution, we can find a better solution. To address the intractability of the model, we use optimization theory and improved MDR to reformulate original model to MILP. Experiments are carried out to show the superiority and availability of the proposed model. Although the proposed model had significant impact on optimizing solutions under uncertainty, there is still room for further improvement: In this paper, we do not consider reduce the number of observed periods that the scheduling scheme relies on, which greatly increases the computational burden of the model and the periods far apart are meaningless to the scheduling scheme in actual scheduling.

REFERENCES

[1] J. Zhu, Optimization of Power System Operation, NJ, Hoboken:Wiley, 2015.

[2] F. Bouffard and F. D. Galiana, "Stochastic Security for Operations Planning With Significant Wind Power Generation," *IEEE Trans. Power Syst.*, vol. 23, no. 2, pp. 306-316, May 2008.

[3] T. Chen, Y. Song, D. J. Hill and A. Y. S. Lam, "Chance-Constrained OPF in Droop-Controlled Microgrids with Power Flow Routers," *IEEE Trans. Smart Grid*, doi: 10.1109/TSG.2022.3154151.

[4] J. Chen, J. Chen and C. Gong, "On optimizing the aerodynamic load acting on the turbine shaft of PMSG-based direct-drive wind energy conversion system", *IEEE Trans. Ind. Electron.*, vol. 61, no. 8, pp. 4022-4031, Aug. 2014.

[5] F. Guo, C. Wen, J. Mao and Y. Song, "Distributed Economic Dispatch for Smart Grids With Random Wind Power," *IEEE Trans. Smart Grid*, vol. 7, no. 3, pp. 1572-1583, May 2016.

[6] Van Ackooij, W, et al. "Large-scale unit commitment under uncertainty: an updated literature survey." *Annals of Operations Research*, vol. 271, no. 1, pp.11-85, 2018.

[7] S. S. Soman, H. Zareipour, O. Malik and P. Mandal, "A review of wind power and wind speed forecasting methods with different time horizons," North American Power Symposium, pp. 1-8, 2010.

[8] H. Y. Su and C. R. Huang, "Enhanced Wind Generation Forecast Using Robust Ensemble Learning," *IEEE Trans. Power Syst.*, vol. 12, no. 1, pp. 912-915, Jan. 2021.

[9] A. Kavousi-Fard, A. Khosravi, and S. Nahavandi, "A new fuzzy-based combined prediction interval for wind power forecasting," *IEEE Trans. Power Syst.*, vol. 31, no. 1, pp. 18–26, Jan. 2016.

[10] C. Peng, P. Xie, L. Pan and R. Yu, "Flexible Robust Optimization Dispatch for Hybrid Wind/Photovoltaic/Hydro/Thermal Power System," *IEEE Trans. Smart Grid*, vol. 7, no. 2, pp. 751-762, March 2016.

[11] R. de Sá Ferreira, L. A. Barroso, P. R. Lino, M. M. Carvalho and P. Valenzuela, "Time-of-Use Tariff Design Under Uncertainty in Price-Elasticities of Electricity Demand: A Stochastic Optimization Approach," *IEEE Trans. Smart Grid*, vol. 4, no. 4, pp. 2285-2295, Dec. 2013.

[12] R. Zhu, H. Wei and X. Bai, "Wasserstein Metric Based Distributionally Robust Approximate Framework for Unit Commitment," *IEEE Trans. Power Syst.*, vol. 34, no. 4, pp. 2991-3001, July 2019.

[13] Xiong, P., Jirutitijaroen, P., Singh, C., 2017. A distributionally robust optimization model for unit commitment considering uncertain wind power generation. *IEEE Trans. Power Syst.*, vol. 32, no. 1, pp. 39-49, Jan. 2017.

[14] L. Yang, Y. Yang, G. Chen and Z. Y. Dong, "Distributionally Robust Framework and Its Approximations Based on Vector and Region Split for Self-scheduling of Generation Companies," *IEEE Trans. Ind. Inform.*, vol. 18, no. 8, pp. 5231-5241, Aug. 2022.

[15] Y. Chen, Q. Guo, H. Sun, Z. Li, W. Wu and Z. Li, "A Distributionally Robust Optimization Model for Unit Commitment Based on Kullback–Leibler Divergence," *IEEE Trans. Power Syst.*, vol. 33, no. 5, pp. 5147-5160, Sept. 2018.

[16] C. Duan, W. Fang, L. Jiang, L. Yao, and L. Jun, "Distributionally robust chance-constrained approximate AC-OPF with Wasserstein metric," *IEEE Trans. Power Syst.*, vol. 33, no. 5, pp. 4924-4936, Sep. 2018.

[17] C. Zhao and Y. Guan, "Data-driven risk-averse stochastic optimization with Wasserstein metric," Oper. Res. Lett., vol. 46, pp. 262-267, 2018.

[18] Á. Lorca, X A Sun, E. Litvinov, T x Zheng, "Multistage Adaptive Robust Optimization for the Unit Commitment Problem," Oper. Res., vol. 64, no. 1, pp. 32-51, 2016.

[19] Y. Zhou, M. Shahidehpour, Z. Wei, G. Sun and S. Chen, "Multistage Robust Look-Ahead Unit Commitment with Probabilistic Forecasting in Multi-Carrier Energy Systems," *IEEE Trans. Sustain. Energy*, vol. 12, no. 1, pp. 70-82, Jan. 2021.

[20] Feng W, Feng Y, Zhang Q, "Multistage distributionally robust optimization for integrated production and maintenance scheduling," AIChE Journal, vol. 67, no. 9, May. 2021.

[21] T. Ding et al., "Multi-Stage Distributionally Robust Stochastic Dual Dynamic Programming to Multi-Period Economic Dispatch With Virtual Energy Storage," *IEEE Trans. Sustain. Energy*, vol. 13, no. 1, pp. 146-158, Jan. 2022.

[22] J. Goh and M. Sim, "Distributionally robust optimization and its tractable approximations," Oper. Res., vol. 58, no. 4, pp. 902–917, 2010.

[23] Garstka S J, Wets J B. "On decision rules in stochastic programming," Math. Program, vol. 7, no. 1, pp.117-143, 1974.

[24] Ben-Tal, A., Goryashko, A., Guslitzer, E., Nemirovski, A,"Adjustable robust solutions of uncertain linear programs," *Math. Program.*, vol. 99, no. 2, pp. 351–376, 2004.

[25] Georghiou, A., Wiesemann, W., & Kuhn, D., "Generalized decision rule approximations for stochastic programming via liftings," *Math. Program.*, vol.152, pp.301–338, 2015.

[26] Delage, E. and Ye, Y. "Distributionally robust optimization under moment uncertainty with application to data-driven problems," *Oper. Res.*, vol. 58, no. 3, pp. 595-612, 2010.

[27] Chao Shang, Fengqi You. Distributionally robust optimization for planning and scheduling under uncertainty. Computers and Chemical Engineering, 110: 53-68. 2018.

[28] Meysam Cheramin, Jianqiang Cheng, Ruiwei Jiang, Kai Pan. "Computationally efficient Approximations for Distributionally Robust Optimization," Opt online, 2020.

[29] C. Zhao, J. Wang, and J. Watson, "Multi-stage robust unit commitment considering wind and demand response uncertainties," *IEEE Trans. Power Syst.*, vol. 28, no. 3, pp. 2708-2717, Aug. 2013.

[30] Dyer,M., Stougie, L.:Computational complexity of stochastic programming problems. *Math. Program.*, 106(3), 423–432 (2006)

[31] Bertsimas D J., Georghiou A., "Binary decision rules for multistage adaptive mixed-integer optimization," *Math. Program.*, vol. 167, no. 3, pp. 1-39, 2017.

[32] All IEEE test system (6 bus-118 bus). [Online]. Available: https://icseg.iti.illinois.edu/power-cases/.

[33] All datas and codes in this paper. [Online]. Available: https://github.com/linfengYang/Fully-Adaptive-Distributionally-Robust-Multi-stage-Framework-for-Uncertain-Unit-Commitment-Based-on/.